Experimental and numerical study of the intermittency exponent μ

By Alexander Praskovsky[1]

1. Motivation, background, and objectives

After publication of the Kolmogorov (1962) refined similarity hypotheses, the small-scale intermittency of the energy dissipation field became a central problem in fully developed turbulence (FDT). This phenomena has been studied in many different ways, e.g. by searching for corrections to scaling exponents in the inertial range velocity structure functions (see reviews in Monin & Yaglom 1975, Kuznetsov & Sabelnikov 1990). A direct measure of this intermittency is, however, available by studying the local rate of energy dissipation, and it may be quantitatively characterized by the intermittency exponent μ (Nelkin 1981).

The first description of the intermittent field was proposed by Kolmogorov (1962), who introduced the energy dissipation ε_r averaged over a segment r:

$$\varepsilon_r(x) \;=\; \frac{1}{r}\int\limits_0^r \varepsilon(x+\chi)d\chi, \tag{1}$$

where x is the longitudinal coordinate, and the local value of the energy dissipation $\varepsilon(x)$ is defined in the standard way as

$$\varepsilon(x) \;=\; \frac{\nu}{2}\Big(\frac{\partial u_i}{\partial x_j} \;+\; \frac{\partial u_j}{\partial x_i}\Big)^2, \tag{2}$$

where ν is the kinematic viscosity, and u_i, $i = 1, 2, 3$, denote the velocity components in the directions x_i. To analyze experimental data and compare them with numerical modeling, the one-dimensional sections of the energy dissipation field in the $x \equiv x_1$ direction will be considered throughout this paper.

It was assumed by Kolmogorov that ε_r has the normal probability density distribution (pdd) if r belongs to the inertial range, i.e., $\eta \ll r \ll L$ where L and η denote the integral and Kolmogorov viscous scales, respectively. This assumption is known as the log-normal model. Kolmogorov further assumed that the variation of $\ln \varepsilon_r$ obeys a logarithmic scaling

$$\sigma^2_{\ln \varepsilon_r} \;=\; A \;+\; \mu_k \,\ln(L/r), \qquad \eta \ll r \ll L, \tag{3}$$

where A is some function of the local flow conditions, and μ_k is the intermittency exponent which was assumed to be a universal constant (if there is no intermittency,

1 National Center for Atmospheric Research, Boulder, Colorado 80307-3000

$\mu_k \equiv 0$). Different subscripts to μ are adopted to identify different definitions of the intermittency exponent.

Novikov & Stewart (1964) showed that

$$< \varepsilon_r^2(x) > \propto r^{-\mu_\varepsilon}, \qquad \eta \ll r \ll L. \tag{4}$$

Hereafter the angular brackets denote average over x. Novikov (1990) demonstrated that under some weak assumptions $\mu_k = \mu_\varepsilon$.

It was also found (Monin & Yaglom 1975) that the correlation function of energy dissipation $R_\varepsilon(r)$ obeys the power-law scaling at separations r within the inertial range

$$R_\varepsilon(r) \equiv < \varepsilon(x)\, \varepsilon(x+r) > = C_\varepsilon < \varepsilon >^2 (r/L)^{-\mu_r}, \qquad \eta \ll r \ll L, \tag{5}$$

where C_ε is assumed to be a universal constant, and $\mu_r = \mu_\varepsilon$.

Monin & Yaglom (1975) further assumed that at very high Reynolds numbers, where fluctuations of $\varepsilon(x)$ are much larger than $< \varepsilon >$,

$$R_\varepsilon(r) \approx B_\varepsilon(r) \equiv < [\varepsilon(x) - < \varepsilon >]\, [\varepsilon(x+r) - < \varepsilon >] > \propto r^{-\mu_b}, \qquad \eta \ll r \ll L, \tag{6}$$

and the energy spectrum of ε (which is the Fourier transform of B_ε) should behave as

$$E_\varepsilon(k) = \frac{1}{\pi} \int_0^\infty B_\varepsilon(r)\, \cos(kr)\, dr \propto k^{-1+\mu_e}, \qquad 1/L \ll k \ll 1/\eta, \tag{7}$$

where k is the wave-number.

Relations (3)–(7) are commonly used to estimate μ. Several more methods for such an estimate are also well-known, e.g. by using the six-order velocity structure function (Monin & Yaglom 1975), the breakdown coefficients (Novikov 1990), etc. but in this brief paper only methods based on (3)–(7) are considered.

A diverse body of measurements of μ in different laboratory flows as well as in the atmosphere and ocean has been reported during the last three decades (for comprehensive review see Kuznetsov & Sabelnikov 1990, Gibson 1991, Nelkin 1994). The reported values of μ vary from 0.15 to 0.7, and this scatter certainly exceeds the measurement errors. Some theoretical considerations as well as the scatter in experimental results caused a doubt about universality of the exponent μ (e.g., Kraichnan 1974, Nelkin 1994). However, as far as we know, nobody has posed an obvious question: Is the intermittency exponent μ **a unique** constant, i.e., are the values μ_k, μ_ε, μ_r, μ_b, and μ_e the same at high Reynolds numbers, or do they create a set of different (and perhaps independent) exponents? This paper addresses the above question using the high Reynolds number experiments.

The second objective of this paper becomes clear from the following considerations. It is commonly assumed (e.g., Monin & Yaglom 1975, Nelkin 1981) that the

longitudinal component $\partial u/\partial x$ should contain most of the important dynamical information on the dissipation field. In other words, it is assumed that the exponents μ defined by Eqs. (3)–(7) would not be changed if the true local rate of energy dissipation $\varepsilon(x)$ were replaced by the one-dimensional surrogate

$$\tilde{\varepsilon}(x) \;=\; 15\,\nu\,(\partial u/\partial x)^2. \tag{8}$$

Nelkin (1981) commented, "this rather weak assumption seems plausible, but is difficult to test experimentally". We are not so optimistic about the "weakness" of this assumption. Indeed, it is well-known (e.g., Hosokawa and Yamamoto 1991) that pdd of $\varepsilon(x)$ and $\tilde{\varepsilon}(x)$ are qualitatively different. The second statement, namely "difficult to test experimentally", is completely valid. In most experiments nothing more than $u(x)$ has been recorded, and in some experiments simultaneous measurements of $u(x)$ and $u_2(x)$ were executed. There are also a few experiments at low Reynolds numbers (see Tsinober *et al.* 1992, and references therein) where all terms in Eq. (2) were directly measured with multi-wire probes. However, the reliability of such measurements, especially at high Reynolds numbers, still seems to be rather questionable.

The remarkable success of direct numerical simulations (DNS) of FDT during the last decades offers another approach to such a test. In spite of well-known limitations (relatively low Reynolds numbers, somewhat arbitrary boundary conditions, etc.), DNS provides an exact solution of the Navier-Stokes equations and gives complete information on the three-dimensional flow field. Using the numerical data base, one can estimate (at least qualitatively) how adequately the true energy dissipation $\varepsilon(x)$ is represented by the one-dimensional surrogate $\tilde{\varepsilon}(x)$. To execute such a test is a second objective of this paper. This approach contradicts traditional belief that measurements give the "final truth", and any theoretical or numerical result should be tested by comparison with experiment. We believe that numerical modeling (now fairly called numerical experiment) becomes so powerful and reliable that it can be used to test physical experiments. First results from this approach are reported in this paper.

2. Accomplishments

2.1 Experimental and numerical data bases

The experimental data base includes measurements in the atmospheric surface layer and in a large wind tunnel at very high Reynolds numbers.

The experiment in the atmospheric surface layer was executed by Dr. Steven Oncley from the National Center for Atmospheric Research (Oncley 1992). After preliminary processing, six time series were chosen from the total record (Praskovsky & Oncley 1994a). Four of these series are analyzed in the present work. The second experiment was executed in the large wind tunnel of the Central Aerohydrodynamic Institute (Moscow, Russia). Measurements have been done in the mixing layer and in the return channel of the wind tunnel (Praskovsky *et al.* 1993).

The main flow characteristics of the experimental data base are listed in Table 1 where the abbreviations ML, RC, and ASL denote the mixing layer, return channel,

and atmospheric surface layer, respectively, and numerals after ASL correspond to the sequence of the time series (in accordance with that in Praskovsky & Oncley 1994a). U is the mean longitudinal velocity, and σ_ϕ denotes the rms value of any quantity ϕ. The Taylor λ and Kolmogorov η scales, and the Reynolds number R_λ, are defined with standard formulas: $\lambda = \sigma_u/\sigma_{\partial u/\partial x}$, $\eta = (\nu^3/ < \varepsilon >)^{1/4}$, and $R_\lambda = \sigma_u \lambda/\nu$. Other quantities in Table 1 will be defined later. Taylor's hypothesis was used to convert from temporal to spatial coordinates.

Time series	ML	RC	ASL-2	ASL-3	ASL-5	ASL-6
U, m/s	7.87	10.8	6.58	8.10	12.9	14.5
σ_u, m/s	1.67	1.03	0.693	1.10	1.82	2.08
L, m	1.3	4.8	42	51	99	77
$< \varepsilon >$, m^2/s^3	1.90	0.115	0.0235	0.0322	0.140	0.128
λ, cm	1.8	4.6	6.5	9.0	7.0	8.3
$R_\lambda \times 10^{-3}$	2.0	3.2	3.3	6.9	9.2	12.7
η, mm	0.21	0.41	0.58	0.55	0.37	0.37
$\overline{\mu_r} \pm \sigma_{\mu_r}$	0.20±0.01	0.19±0.01	0.20±0.01	0.20±0.01	0.20±0.02	0.20±0.01
$\overline{\mu_b} \pm \sigma_{\mu_b}$	0.38±0.01	0.32±0.01	0.35±0.02	0.29±0.03	0.33±0.02	0.30±0.02
$\overline{\mu_e} \pm \sigma_{\mu_e}$	0.59±0.03	0.60±0.02	0.57±0.04	0.61±0.02	0.56±0.02	0.55±0.01
$\overline{\mu_k} \pm \sigma_{\mu_k}$	0.40±0.01	0.22±0.03	0.19±0.04	0.22±0.02	0.22±0.02	0.23±0.02
$\overline{\beta} \pm \sigma_\beta$	0.26±0.01	0.24±0.01	0.23±0.02	0.19±0.01	0.18±0.01	0.14±0.01
$\overline{\gamma_\varepsilon} \pm \sigma_{\gamma_\varepsilon}$	0.42±0.01	0.38±0.01	0.41±0.02	0.38±0.01	0.36±0.01	0.35±0.01

Table 1. Main turbulence characteristics of analyzed time series.

The DNS of homogeneous, isotropic, equilibrium flow fields were executed by Dr. Robert Rogallo from the NASA Ames Research Center. A description of this data base, covering a range of R_λ from 35 to 168 can be found in Jimenez *et al.* (1993). Two simulations at $R_\lambda = 94$ and 168 are analyzed in the present work.

2.2 Experimental results for $\tilde{\varepsilon}(x)$

2.2.1 Correlation functions and spectra

Two examples of the correlation functions $R_\varepsilon(r)$ and $B_\varepsilon(r)$ at the lowest and highest R_λ are presented in Fig. 1. The local values of scaling exponents are estimated using the logarithmic derivatives:

$$\mu_r(r) = -\frac{d[\lg R_\varepsilon(r)]}{d[\lg r]}, \quad \mu_b(r) = -\frac{d[\lg B_\varepsilon(r)]}{d[\lg r]}, \quad \mu_e(k) = 1 + \frac{d[\lg E_\varepsilon(k)]}{d[\lg k]}. \tag{9}$$

It follows from Eqs. (5)–(7) that μ_r, μ_b, and μ_e should be constants within the inertial range. The measured values of $\mu_r(r)$ and $\mu_b(r)$ are presented in Fig. 2. The constant-value regions of these exponents are ill-defined, especially for $\mu_b(r)$. However, for each time series one can choose a range of separations r where the exponents are *approximately* constant. Within these limits, deviations of μ from constant can be attributed to measurement uncertainty. The mean values $\overline{\mu_i}$ and

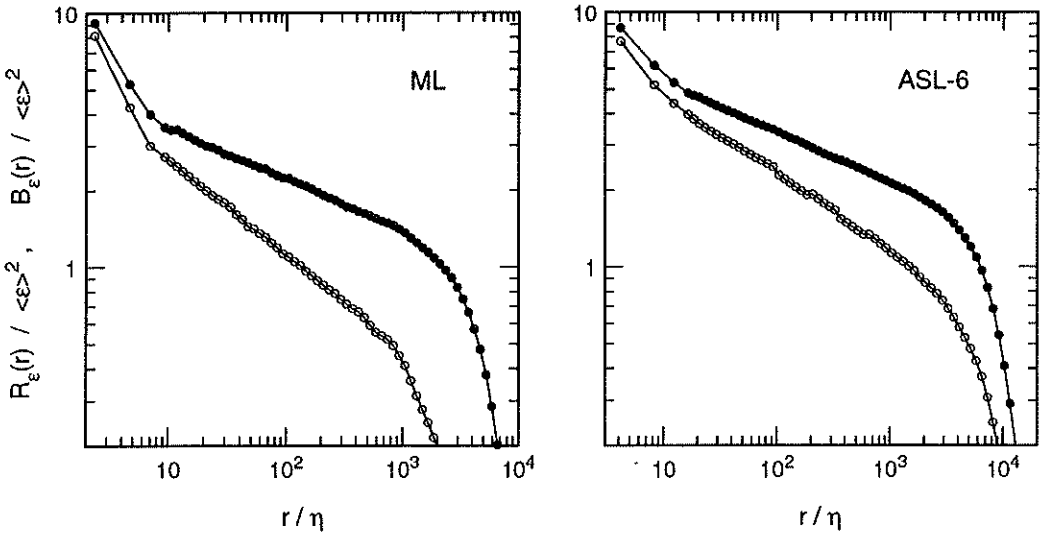

FIGURE 1. Correlation functions of the energy dissipation. •, $R_\varepsilon(r)$; ○, $B_\varepsilon(r)$.

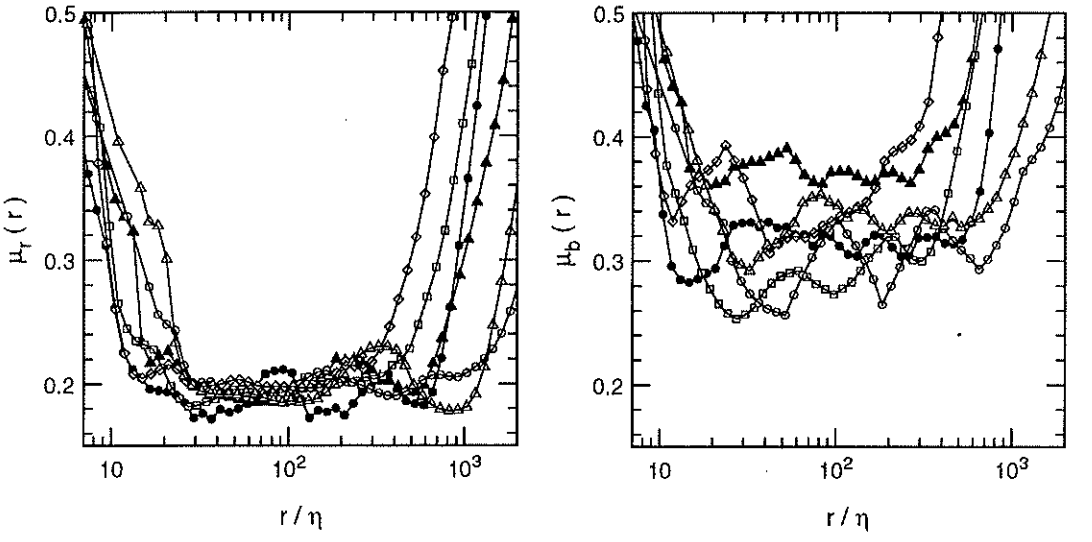

FIGURE 2. The local values of scaling exponents $\mu_r(r)$ and $\mu_b(r)$. Note the expanded linear scale of the ordinate at this and other similar figures. ▲, ML; •, RC; ◇, ASL-2; □, ASL-3; △, ASL-5; ○, ASL-6.

standard deviations σ_{μ_i}, $(i = r, b)$ were estimated by averaging over these ranges, and the results are listed in Table 1. It is seen that $\overline{\mu_r}$ is significantly smaller than $\overline{\mu_b}$. This result is not surprising. Anselmet *et al.* (1984) found $\mu_r = 0.18$ and $\mu_b = 0.48$ in the round jet at $R_\lambda = 536$. Kuznetsov *et al.* (1992) found $\mu_r \approx 0.14$, $\mu_b \approx 0.45$, and $\mu_e \approx 0.60$ in the mixing layer at $R_\lambda \approx 1700$. The equality $R_\varepsilon(r) \approx B_\varepsilon(r)$ is based on the assumption that both $R_\varepsilon(r)$ and $B_\varepsilon(r)$ are much larger than $< \varepsilon >^2$

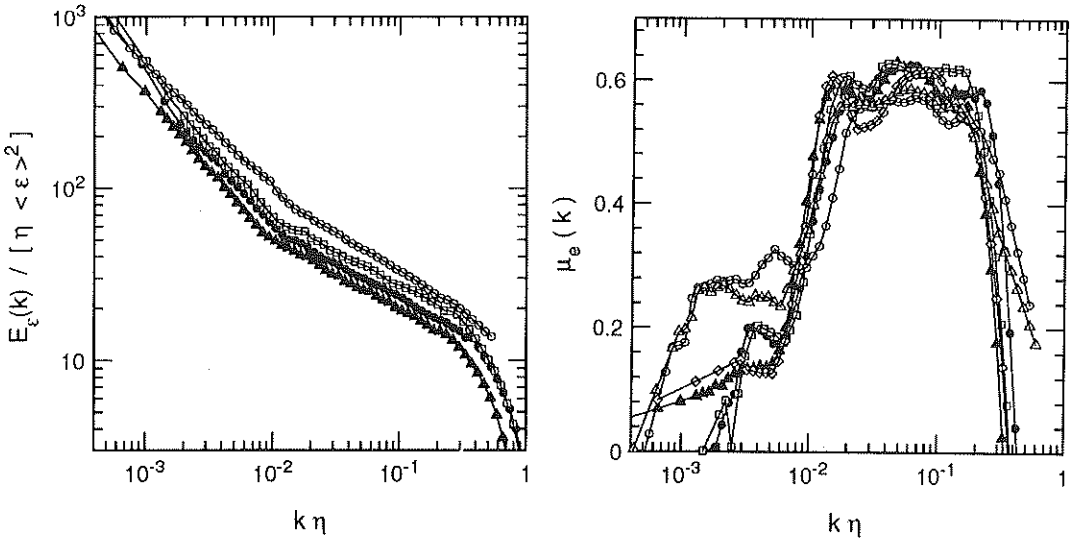

FIGURE 3. Spectra of the energy dissipation, and the local values of scaling exponent $\mu_e(k)$. For symbols see Fig. 2.

in the inertial range (Monin & Yaglom 1975). This assumption is not valid *at any finite Reynolds number*. It is seen in Fig. 1 that at big enough r, say at $r/\eta \approx 10^3$, $B_\varepsilon(r)$ is smaller than $< \varepsilon >^2$. Hence one should always obtain $\mu_r < \mu_b$. There is a contradiction, recently noted by Praskovsky & Oncley (1994b). The correlation functions are connected by the exact relation:

$$B_\varepsilon(r) \equiv R_\varepsilon(r) - < \varepsilon >^2 . \tag{10}$$

It obviously follows from this relation that at any finite R_λ where $< \varepsilon >^2$ is of the order of (or even larger than) $B_\varepsilon(r)$ at $\eta \ll r \ll L$, only one of the functions, $R_\varepsilon(r)$ or $B_\varepsilon(r)$, may obey the power-law scaling. As was mentioned above, the constant-value regions for both $\mu_r(r)$ and $\mu_b(r)$ are ill-defined. Taking into consideration Eq. (10), one can suggest that the present experiments as well as all previous measurements *do not prove* power-law behavior of any correlation function. The results demonstrate that the power laws (5) and (6) *reasonably approximate* both correlators within the inertial range.

Typical energy spectra $E_\varepsilon(k)$ and local values of the scaling exponents $\mu_e(k)$ are presented in Fig. 3. It is seen that at large enough k the power law (7) gives reasonable approximation of $E_\varepsilon(k)$. The mean values $\overline{\mu_e}$ and the standard deviation σ_{μ_e} are estimated over the ranges where $\mu_e(k)$ are approximately constant, and the results are listed in Table 1. It is seen that $\overline{\mu_e}$ are roughly twice $\overline{\mu_b}$. This result agrees with previous studies, and it is explained by Nelkin (1981). It follows from Eq. (7) that $\mu_b \equiv \mu_e$ if scaling (6) is valid for all r from 0 to infinity. In reality, $B_\varepsilon(0)/ < \varepsilon >^2$ increases with no limit as $R_\lambda \to \infty$ while the inertial range values of $B_\varepsilon(r)/ < \varepsilon >^2$ increase more slowly. In other words, $B_\varepsilon(r)$ has a strong peak at $r \leq \eta$, and this peak increases as R_λ increases. As was shown by Kuznetsov

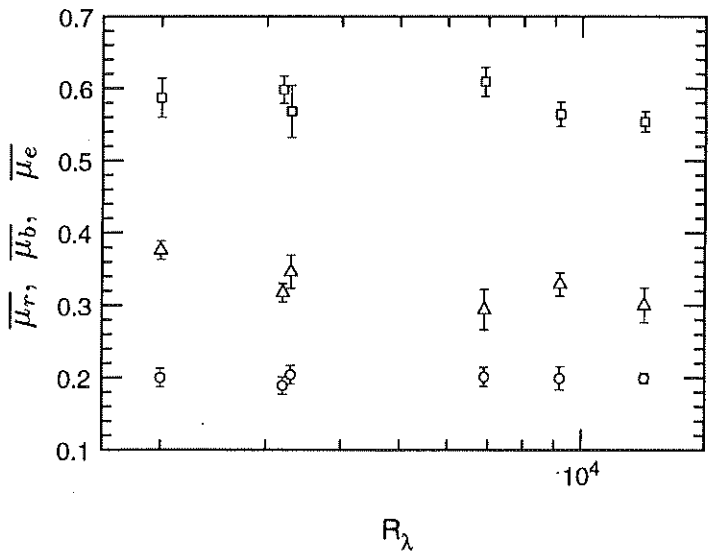

FIGURE 4. Scaling exponents averaged over the inertial range.
Error bars at this and other similar figures correspond to the rms value of the exponent. ○ , $\overline{\mu_r}$; △ , $\overline{\mu_b}$; □ , $\overline{\mu_e}$.

et al. (1990), μ_b is always smaller than μ_e, and this difference may increase when R_λ increases.

The values of $\overline{\mu_r}$, $\overline{\mu_b}$, and $\overline{\mu_e}$ are plotted in Fig. 4. Beyond any doubt, μ_r, μ_b, and μ_e are different exponents at R_λ up to 12,700. Variation of these exponents with R_λ and the type of flow is quite small. As a first approximation, one can consider the exponents $\mu_r \approx 0.2$, $\mu_b \approx 0.3$, and $\mu_e \approx 0.55$ to be universal (but different!) constants at the highest Reynolds numbers currently attainable, say at $R_\lambda \geq 2\times10^3$. At Reynolds numbers too high to be attained on this planet, the different μ's could still be the same.

2.2.2 Test of the log-normal model

The log-normal model includes the statement that $\ln \varepsilon_r$ has a normal distribution for $\eta \ll r \ll L$ (Kolmogorov 1962). Note that this assumption and Eq. (3) are two *independent* hypotheses, i.e., the log-normal model may be valid while Eq. (3) is not, and vice-versa (see Castaing *et al.* 1990 for more explanation).

The log-normality of $\ln \varepsilon_r$ was tested in numerous experiments (see reviews in Monin & Yaglom 1975, Gibson 1991), and this was found to give a reasonable approximation of reality in different turbulent flows. The present experiments give similar results. As an illustration, several distributions for segments r from the inertial range are presented in Fig. 5. It is surprising that deviations of experimental results from the log-normal model increase as R_λ increases.

Eq. (3) was also reported by many authors to be valid (see Gibson 1991 and references therein). However, Castaing *et al.* (1990) presented experimental and theoretical evidences that at small r (up to the viscous range) the variation of $\ln \varepsilon_r$ obeys the power-law scaling

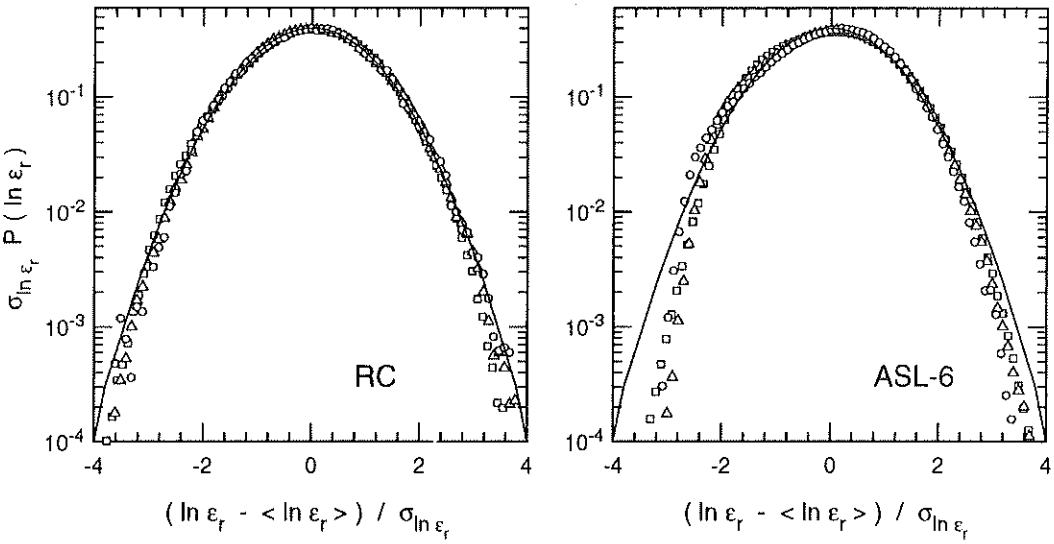

FIGURE 5. Pdd of $\ln \varepsilon_r$. Solid lines correspond to the normal distribution. RC: □ , $r/\eta = 23$; △ , 130; ○ , 927; ASL-6: □ , $r/\eta = 33$; △ , 180; ○ , 1025.

$$\sigma^2_{\ln \varepsilon_r} \propto r^{-\beta}. \tag{11}$$

Hypotheses (3) and (11) are tested in Fig. 6. The local values of $\mu_k(r)$ and $\beta(r)$ are defined as

$$\mu_k(r) = -\frac{d[\sigma^2_{\ln \varepsilon_r}]}{d[\ln r]}, \qquad \beta(r) = -\frac{d[\lg \sigma^2_{\ln \varepsilon_r}]}{d[\lg r]}. \tag{12}$$

It is seen that at large r, say $r/\eta \geq 200$, the Kolmogorov (1962) assumption (3) provides a good approximation of the experimental results. At small r Eq. (3) does not agree with the present experiments while the power-law scaling (11) works quite well. The values of $\overline{\mu_k}$ and $\overline{\beta}$ averaged over regions where they are approximately constant are listed in Table 1 and presented in Fig. 7. One can see that μ_k does not depend on R_λ and the type of flow at $R_\lambda \geq 3 \times 10^3$, and is approximately equal to 0.22. The exponent β in (11) does not reveal any dependence on the type of flow (measurements by Castaing *et al.* 1990 in the round jet at $R_\lambda = 852$ and in the Modane wind tunnel at $R_\lambda = 2720$ are also presented in Fig. 7). However, this exponent strongly depends on R_λ, and the dependence may be approximated as $\beta \propto R_\lambda^{-1/3}$, which is different from the relation $\beta \propto 1/\ln R_\lambda$ suggested by Castaing *et al.* (1990).

2.2.3 Measurements of the second-order moments

The measured values of $< \varepsilon_r^2(x) >$ as well as the local values of scaling exponent $\mu_\varepsilon(r) = -d[\lg < \varepsilon_r^2 >]/d[\ln r]$ are presented in Fig. 8. No region of power-law scaling is seen within the inertial range; i.e., $\mu_\varepsilon(r)$ decreases monotonically over the range of r/η from say 5 to 20,000. Contradiction of this result to all previous studies is

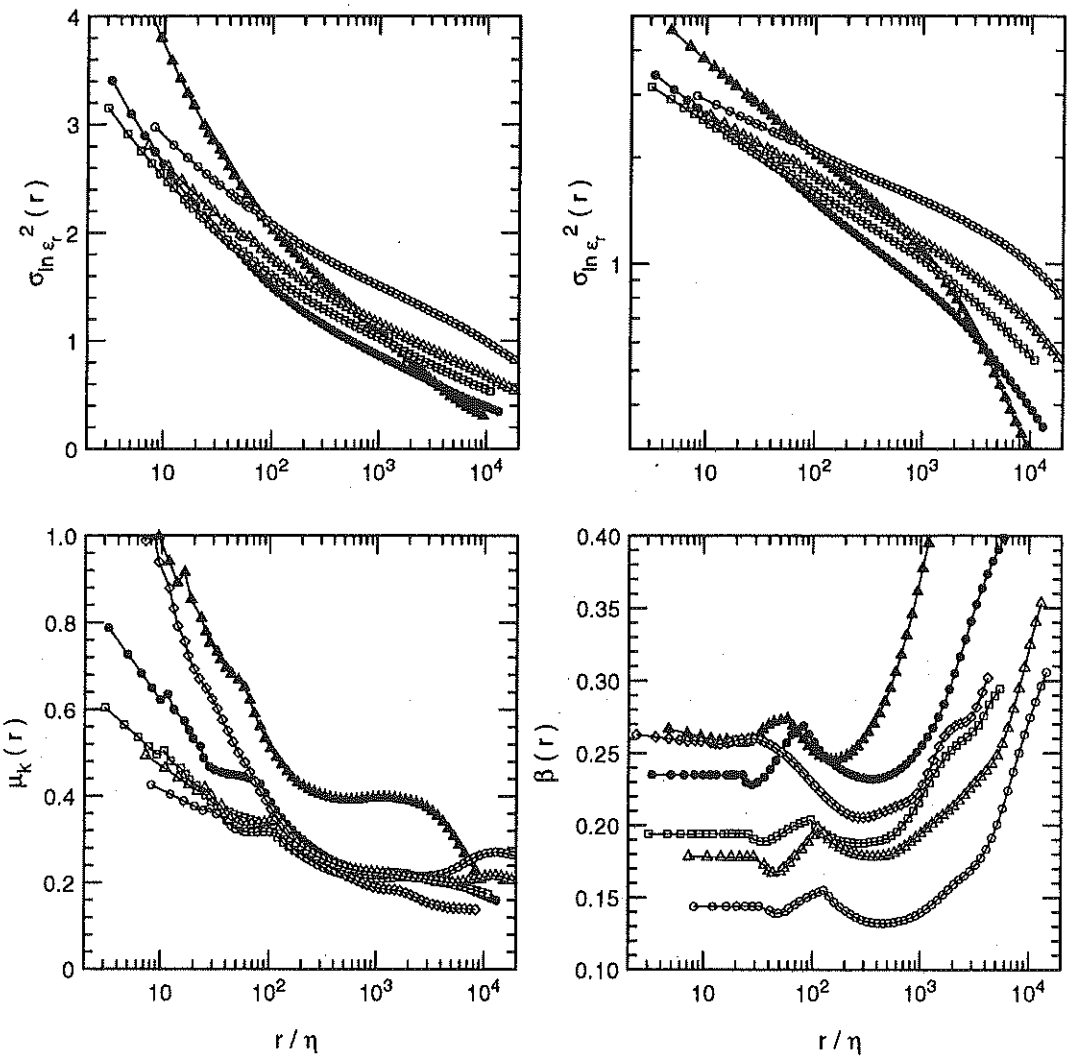

FIGURE 6. Variation of $\ln \varepsilon_r$, and the local values of $\mu_k(r)$ and $\beta(r)$.

apparent. No previous papers reported the local values $\mu_\varepsilon(r)$, but only log-log plots such as that in Fig. 8. Such plots may be deceptive; a range of slow change in $\mu_\varepsilon(r)$ may be erroneously considered as implying $\mu_\varepsilon(r) \approx$ constant.

It was recently suggested by L'vov and Procaccia (1994) that scaling (4) should be applied to the centered second-order moment, i.e., the relation

$$< [\varepsilon_r(x) - < \varepsilon >] >^2 \propto r^{-\gamma_\varepsilon}, \qquad \eta \ll r \ll L \tag{13}$$

should be used instead of (4). This suggestion is tested in Fig. 9. It is seen that $\gamma_\varepsilon(r) = d[\lg < (\varepsilon_r - < \varepsilon >)^2 >]/d[\ln r]$ does reveal some range of being approximately constant. The values of $\overline{\gamma_\varepsilon}$ averaged over these ranges are presented in Fig. 10. It is seen that γ_ε slightly depends on Reynolds number.

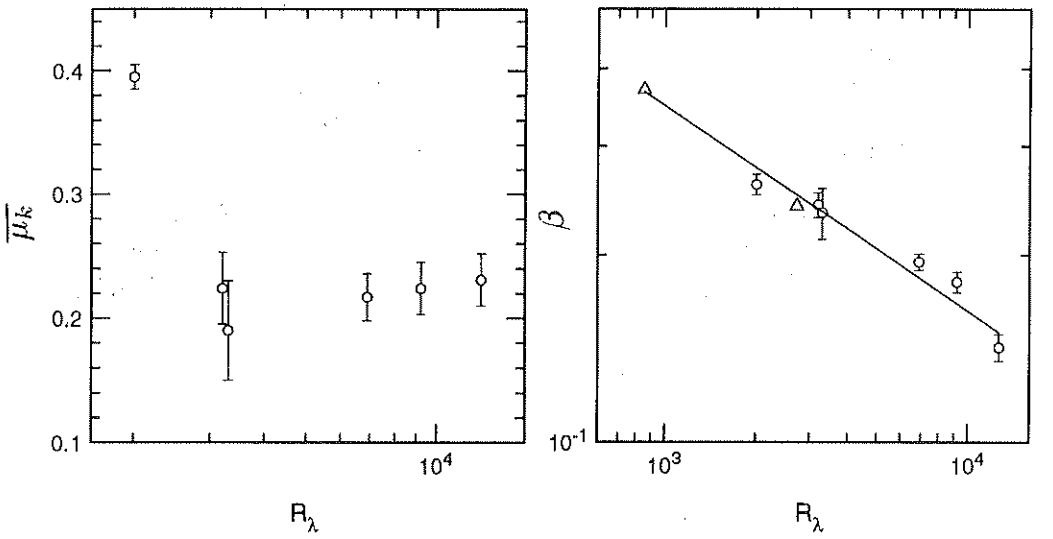

FIGURE 7. Averaged values of the exponents $\overline{\mu_k}$ and $\overline{\beta}$. ——— corresponds to $\beta \propto R_\lambda^{-1/3}$; o , the present results; △ , Castaing *et al.* (1990).

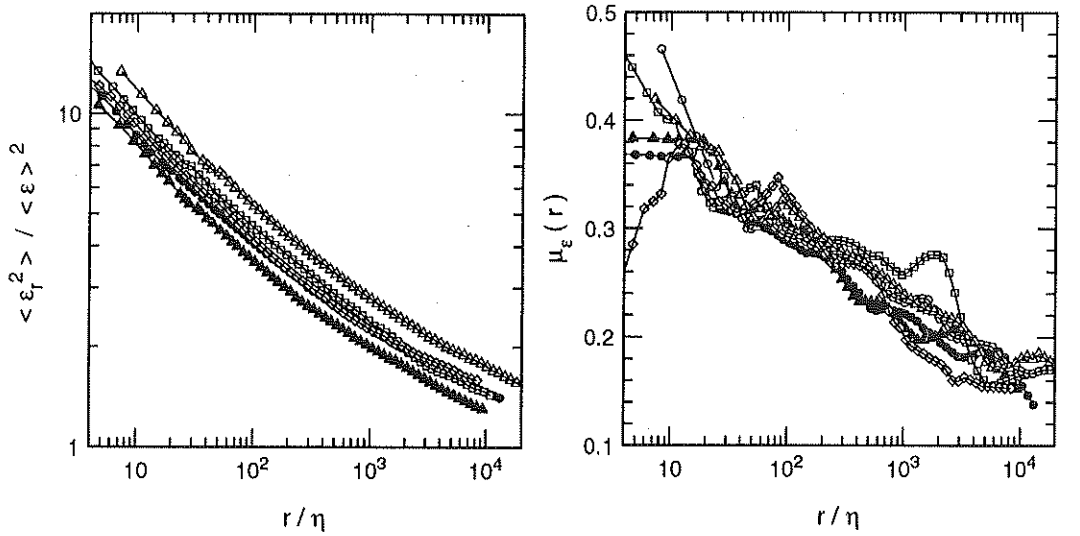

FIGURE 8. The second-order moments $< \varepsilon_r^2(x) >$ and the local values of scaling exponent $\mu_\varepsilon(r)$. For symbols see Fig. 2.

2.3 Analysis of the DNS data base

Two DNS of isotropic homogeneous turbulence at $R_\lambda = 94$ and 168 (Jimenez *et al.* 1993) are analyzed. The purpose of this analysis is a comparison of statistical characteristics of the "true" energy dissipation field $\varepsilon(x)$, Eq. (2), and its one-dimensional surrogate $\tilde{\varepsilon}(x)$, Eq. (8). Significance of such a comparison is illustrated in Fig. 11 where pdd $P(\varepsilon)$ of $\varepsilon(x)$ and $P(\tilde{\varepsilon})$ of $\tilde{\varepsilon}(x)$ are presented. One can see a

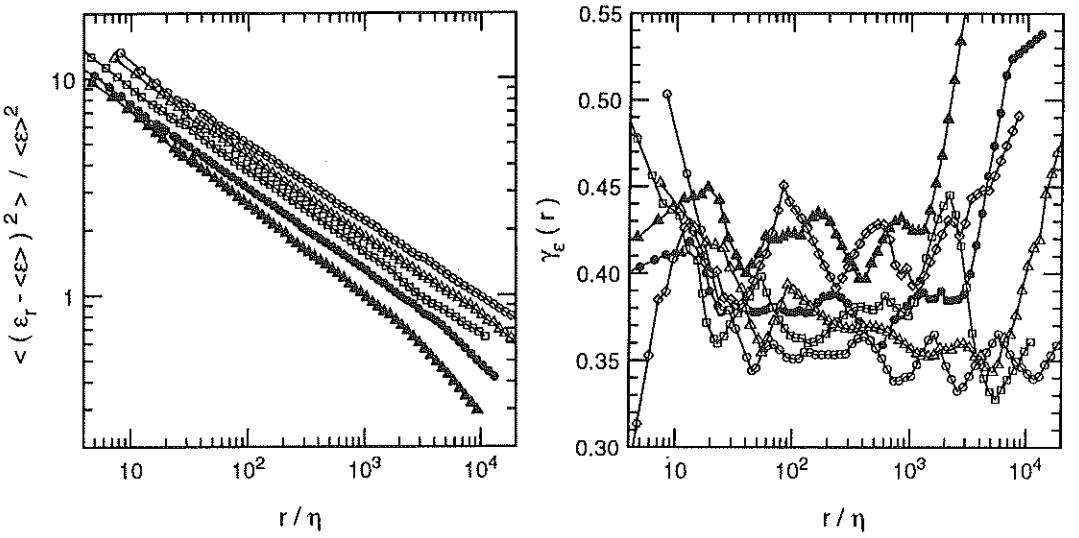

FIGURE 9. The centered second-order moments $< [\varepsilon_r(x) - < \varepsilon_r >]^2 >$, and the local values of scaling exponent $\gamma_\varepsilon(r)$. For symbols see Fig. 2.

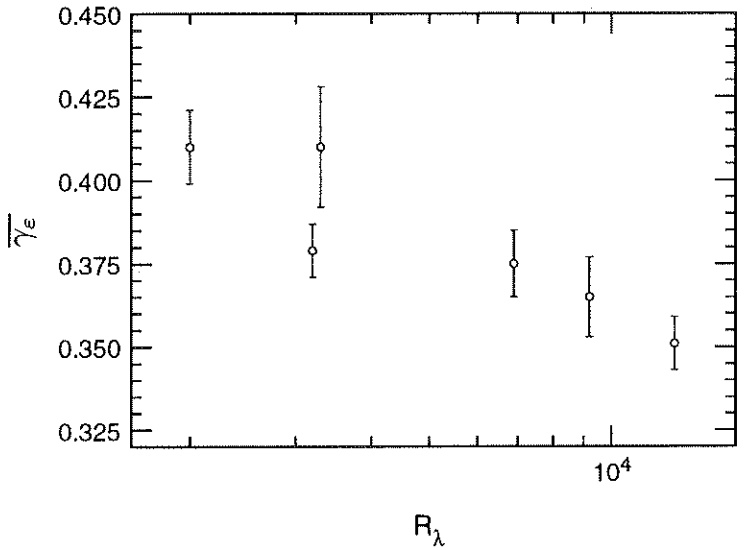

FIGURE 10. Exponent $\overline{\gamma_\varepsilon}$ averaged over the inertial range.

qualitative difference of these functions: $P(\varepsilon) \to 0$ as $\varepsilon \to 0$ while $P(\tilde{\varepsilon}) \to P_0 > 0$ as $\tilde{\varepsilon} \to 0$ (see also Hosokawa and Yamamoto 1991). In other words, we test a question: what of the results from Sec. 2.2 which are obtained for $\tilde{\varepsilon}(x)$ are valid for the true dissipation $\varepsilon(x)$? A comparison is executed in the following way. Using the DNS data base, each parameter is estimated for the true energy dissipation and one-dimensional surrogate by substituting in the same defining formula either $\varepsilon(x)$ or $\tilde{\varepsilon}(x)$, respectively.

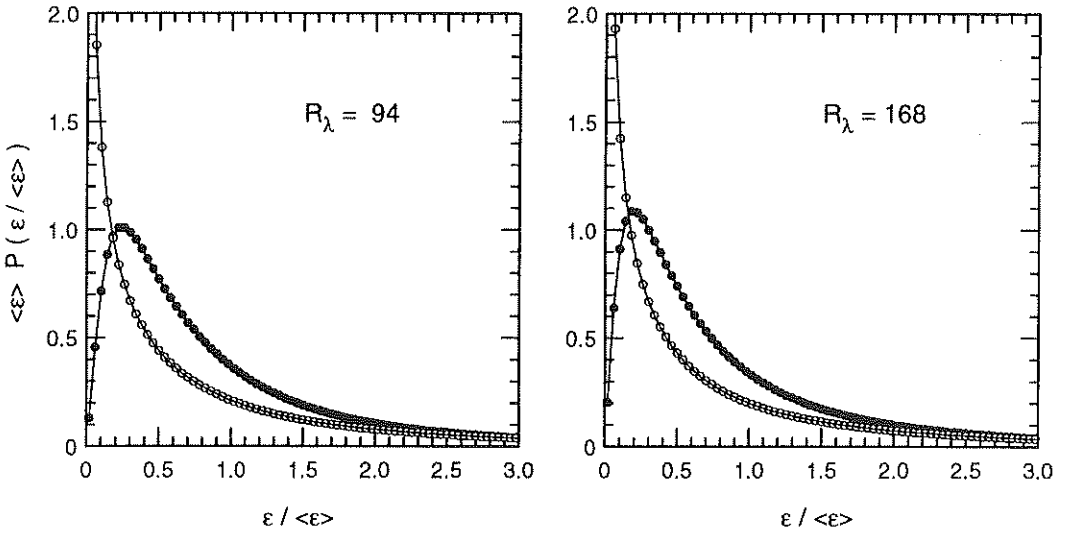

FIGURE 11. DNS: pdd of the energy dissipation. In this and the following figures the solid symbols correspond to the true dissipation $\varepsilon(x)$, and the open symbols correspond to the one-dimensional surrogate $\tilde{\varepsilon}(x)$.

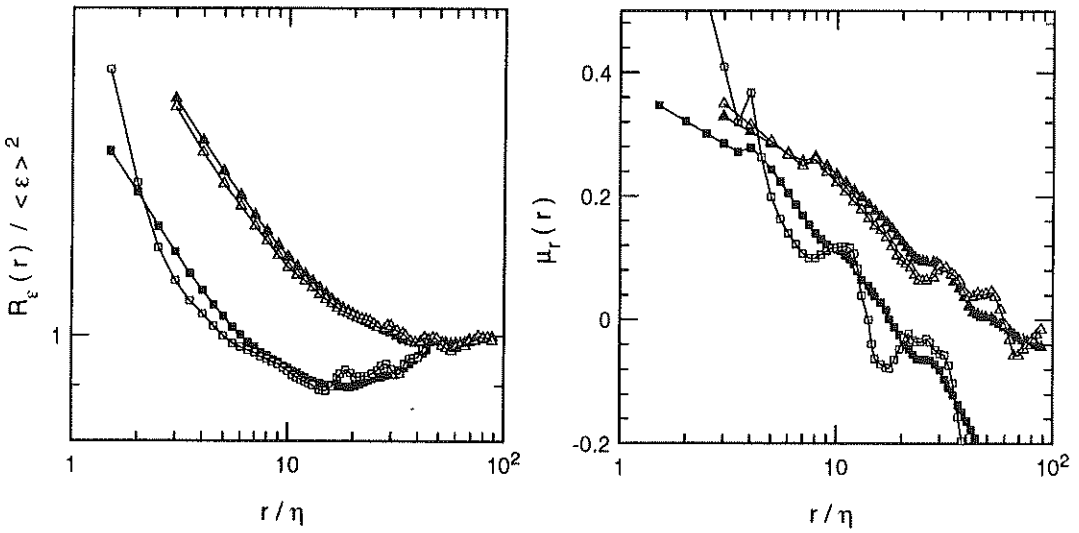

FIGURE 12. DNS: correlation functions of the energy dissipation, and the local values of scaling exponent $\mu_r(k)$. □ , $R_\lambda = 94$; △ , 168. See caption of Fig. 11.

The correlation functions $R_\varepsilon(r)$ and the local values of scaling exponent $\mu_r(r)$ are presented in Fig. 12. No clearly defined inertial range is seen, i.e., there is no region where $\mu_r(r) \approx$ constant. This is expected due to relatively low Reynolds number in the present DNS. In spite of different pdd (Fig. 11), a qualitative behavior of $R_\varepsilon(r)$ for $\varepsilon(x)$ and $\tilde{\varepsilon}(x)$ is quite similar. Hence one can expect that results and conclusions

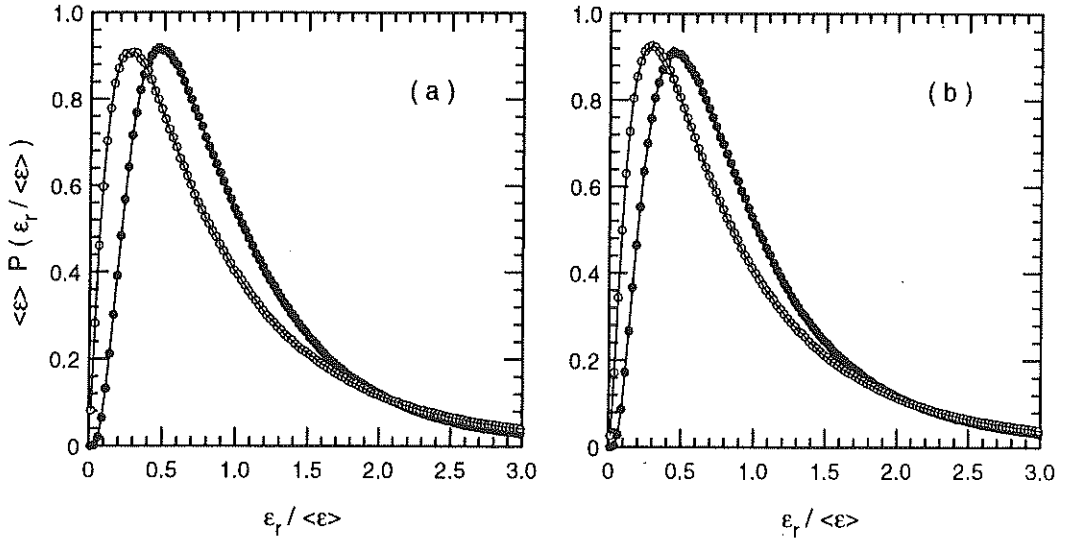

FIGURE 13. DNS: pdd of the energy dissipation averaged over a segment r. (a) $R_\lambda = 94$, $r/\eta = 10$; (b) $R_\lambda = 168$, $r/\eta = 15$. See caption of Fig. 11.

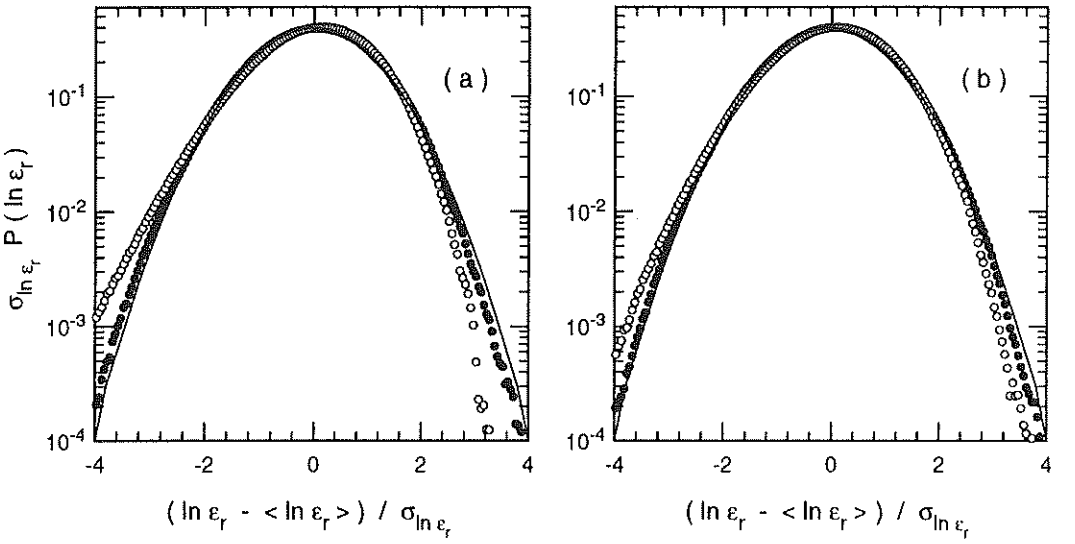

FIGURE 14. DNS: pdd of $\ln \varepsilon_r$. Solid lines correspond to the normal distribution. (a) $R_\lambda = 94$, $r/\eta = 10$; (b) $R_\lambda = 168$, $r/\eta = 15$. See caption of Fig. 11.

of Sec. 2.2.1 are valid for the true energy dissipation field.

Pdd of energy dissipation averaged over a segment r are presented in Fig. 13. Variation of $\tilde{\varepsilon}_r(x)$ is much larger than that of $\varepsilon_r(x)$: the maxima of $P(\tilde{\varepsilon}_r)$ are shifted to the smaller amplitudes while the tails of $P(\tilde{\varepsilon}_r)$ at large amplitudes are higher than those of $P(\varepsilon_r)$. The log-normal model is tested in Fig. 14. The true energy dissipation field agrees quite well with the model while $P(\ln \tilde{\varepsilon}_r)$ reveals significant

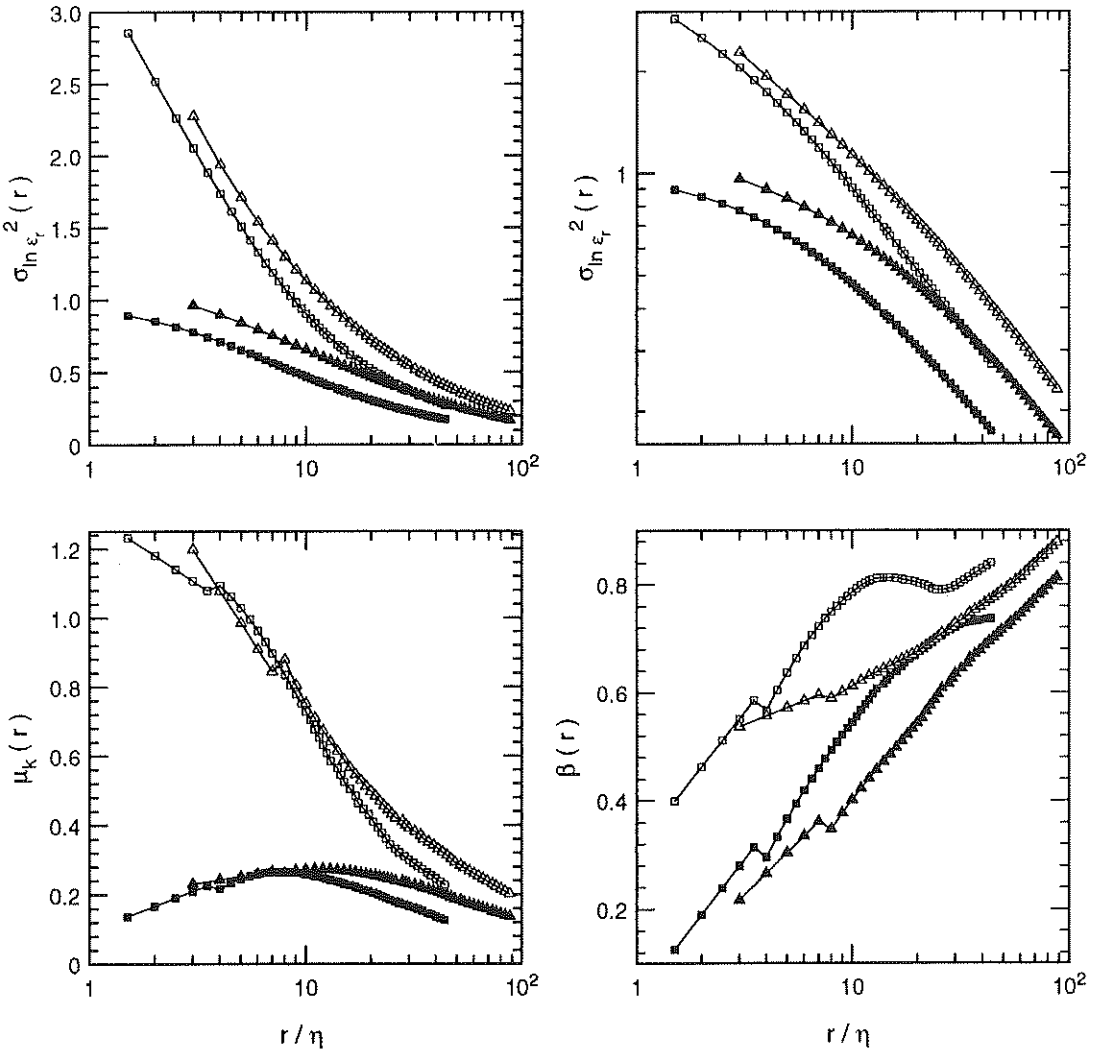

FIGURE 15. DNS: variation of $\ln \varepsilon_r$, and the local values of $\mu_k(r)$ and $\beta(r)$. □, $R_\lambda = 94$; △, 168. See caption of Fig. 11.

deviations similar to those in Fig. 5. One can suggest that the deviations from the log-normal model in Fig. 5 would be smaller (or even disappear) if the true energy dissipation was measured at high R_λ.

Eqs. (3) and (11) were tested, and the results are presented in Fig.15 which is similar to Fig. 6 for experimental data. A qualitative behavior of $\sigma^2_{\ln \varepsilon_r}$ for the one-dimensional surrogate in the DNS is completely similar to that in the high Reynolds number experiments. The DNS results for $\tilde{\varepsilon}_r$ do not agree with Eq. (3) at $r/\eta \approx$ 7–20 (this region is expected to model the inertial range) while they agree with Eq. (11). On the other hand, the true field $\varepsilon_r(x)$ is reasonably described by Eq. (3) in the vicinity of $r/\eta \approx 10$, and it does not agree with Eq. (11). Using DNS at

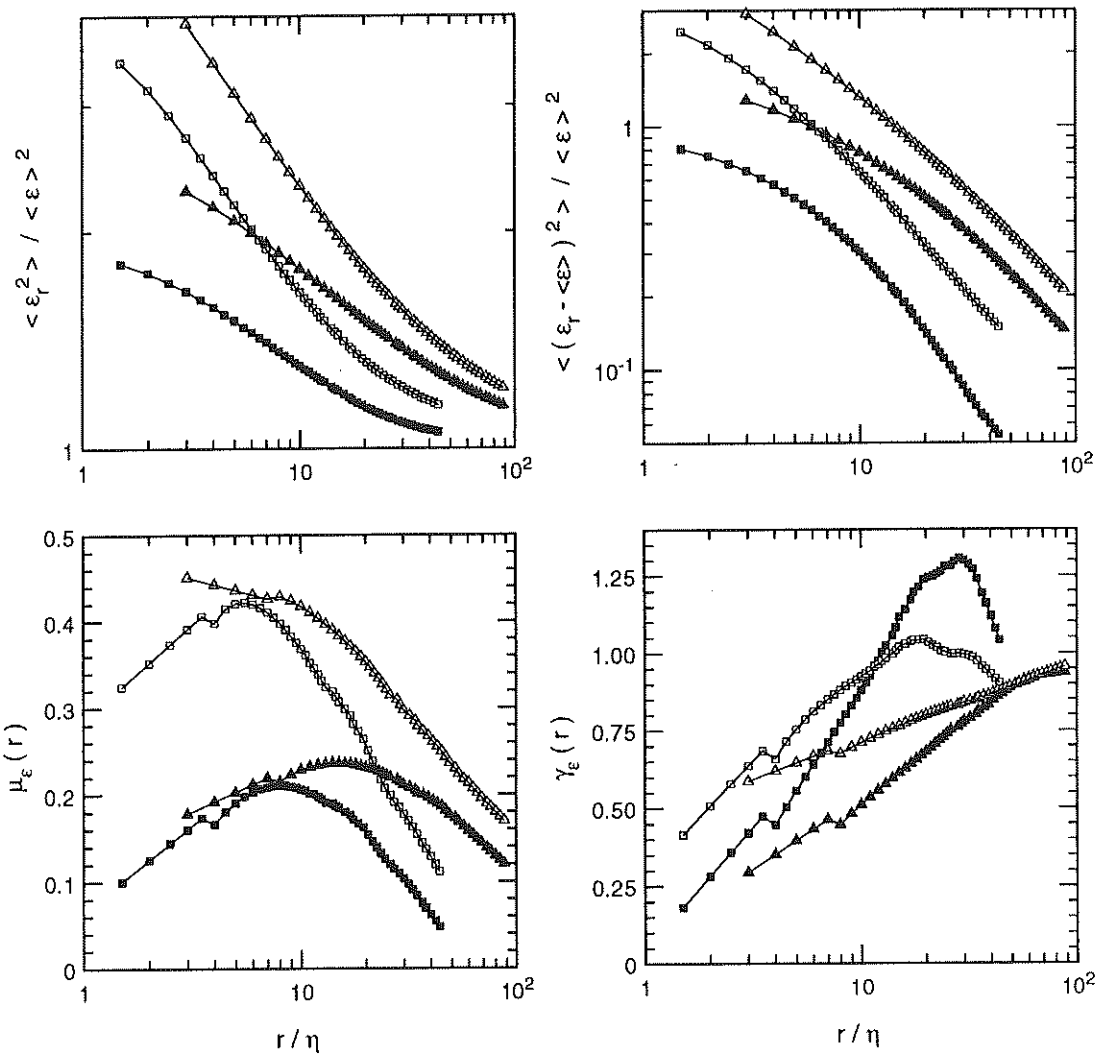

FIGURE 16. DNS: the non-centered and centered second-order moments of $\varepsilon_r(x)$, and the local values of scaling exponents $\mu_\varepsilon(r)$ and $\gamma_\varepsilon(r)$. □ , $R_\lambda = 94$; △ , 168. See caption of Fig. 11.

$R_\lambda = 68.1$ and 151, Wang *et al.* (1994) recently found the values of $\mu_k \approx 0.28$ for the true field $\varepsilon_r(x)$, and 0.34 for the surrogate $\tilde{\varepsilon}_r(x)$. In the present DNS the values of $\mu_k(r)$ for $\tilde{\varepsilon}_r$ are also larger than those for ε_r (Fig. 15). However, our results differ conceptually from those by Wang *et al.* (1994). We state that the surrogate field does not obey Eq. (3) in the vicinity of $r/\eta \approx 10$–15, and no value of μ_k may be estimated. Perhaps, Wang *et al.* (1994) would draw the same conclusion if they used the logarithmic derivatives instead of the log-linear plots of $\sigma^2_{\ln \varepsilon_r}$ *vs* $\ln r$.

The DNS results for $< \varepsilon_r^2 >$ (Fig. 16) are also similar to the experimental data (Figs. 8, 9). A functional behavior of the second-order moment $< \tilde{\varepsilon}_r^2 >$ in the DNS

agrees with Eq. (13) at $r/\eta \approx 10$–20 as that in experiments while $< \varepsilon_r^2 >$ clearly agrees with Eq. (4).

It follows from the above results that the experimental findings of Sec. 2.2.2 and 2.2.3 may be valid only for $(\partial u/\partial x)^2$, and their application to the true dissipation field $\varepsilon(x)$ is quite questionable. Based on these preliminary results, we cannot draw any final conclusions. However, two suggestions may be stated. First, any experimental finding obtained for the surrogate $\tilde{\varepsilon}(x)$ should not be applied to the true dissipation field before similarity of this result to that for $\varepsilon(x)$ is proven. Second, DNS seems to be the most reliable (and perhaps a unique) tool for such a proof.

3. Future plans

The goal remains to understand what characteristics of the energy dissipation field are adequately represented by the one-dimensional surrogate. To further study this question, we are going to use the recent DNS data base with resolution 512^3.

The second question may be formulated as follows: what is the minimum set of terms in Eq. (2) which adequately represents any statistical characteristic of $\varepsilon(x)$? An answer to this question will allow a proper design of the future high Reynolds number experiments.

Acknowledgments

The author is sincerely grateful to Dr. Steven Oncley for the experimental data in the atmospheric surface layer, to Dr. Robert Rogallo for the DNS data base, intensive help, and valuable discussions, and to Prof. Peter Bradshaw for comments on the draft. The experimental part of this work was supported by the National Center for Atmospheric Research, and the computational part by the Center for Turbulence Research. Personal encouragement and valuable comments by Prof. Parviz Moin are highly appreciated.

REFERENCES

ANSELMET, F., GAGNE, Y., HOPFINGER, E. J. & ANTONIA, R. A. 1984 High-order velocity structure functions in turbulent shear flows. *J. Fluid Mech.* **140,** 63-89.

CASTAING, B., GAGNE, Y. & HOPFINGER, E. J. 1990 Velocity probability density functions of high Reynolds number turbulence. *Physica D.* **46,** 177-200.

GIBSON, C. H. 1991 Kolmogorov similarity hypotheses for scalar fields: sampling intermittent turbulent mixing in the ocean and galaxy. *Proc. R. Soc. Lond. A.* **434,** 149-164.

HOSOKAWA, I. & YAMAMOTO, K. 1992 Evidence against the Kolmogorov refined similarity hypothesis. *Phys. Fluids A.* **4,** 457-459.

JIMENEZ, J., WRAY, A.A., SAFFMAN, P.G. & ROGALLO, R.S. 1993 The structure of intense vorticity in isotropic turbulence. *J. Fluid Mech.* **255,** 65-90.

KOLMOGOROV, A. N. 1962 A refinement of previous hypotheses concerning the local structure of turbulence in a viscous incompressible fluid at high Reynolds numbers. *J. Fluid Mech.* **13,** 82-85.

KRAICHNAN, R. H. 1974 On Kolmogorov's inertial-range theories. *J. Fluid Mech.* **62,** 305-330.

KUZNETSOV, V. R., PRASKOVSKY, A. A. & SABELNIKOV, V. A. 1990 Intermittency and fine-scale turbulence structure of shear flows. *Proc. Inst. of Thermo-Physics.* (Novosibirsk, Russia), 223-224.

KUZNETSOV, V. R., PRASKOVSKY, A. A. & SABELNIKOV, V. A. 1992 Fine-scale turbulence structure of intermittent shear flows. *J. Fluid Mech.* **243,** 595-622.

KUZNETSOV, V. R. & SABELNIKOV, V. A. 1990 *Turbulence and Combustion* (Hemisphere Publ.).

L'VOV, V. S. & PROCACCIA, I. 1994 'Intermittency" in hydrodynamic turbulence as an intermediate asymptotic to Kolmogorov'41 scaling. Submitted to *Phys. Rev. Lett.*

MONIN, A.S. & YAGLOM, A.M. 1975 *Statistical Fluid Mechanics,* **2, (MIT Press).**

NELKIN, M. 1981 Do the dissipation fluctuations in high Reynolds number turbulence define a universal exponent? *Phys. Fluids* **24,** 556-557.

NELKIN, M. 1994 Universality and scaling in fully developed turbulence. *Advances in Physics,* in press.

NOVIKOV, E. A. 1990 The effect of intermittency on statistical characteristics of turbulence and scale similarity of breakdown coefficients. *Phys. Fluids A.* **2,** 814-820.

NOVIKOV, E.A. & STEWART, R.W. 1964 The intermittency and the spectral distribution of energy dissipation. *Izv. Akad. Nauk SSSR, Ser. Geofiz.* **2,** 408-413.

ONCLEY, S. 1992 TKE dissipation measurements during the FLAT experiment. In *Proc. of 10th Symp. on Turbulence and Diffusion,* 165-166 (AMS, Boston MA).

PRASKOVSKY, A. A., GLEDZER, E. B., KARYAKIN, M. YU. & ZHOU, Y. 1993 The sweeping decorrelation hypothesis and energy-inertial scale interaction in high Reynolds number flows. *J. Fluid Mech.* **248,** 493-511.

PRASKOVSKY, A. A. & ONCLEY, S. 1994a Measurements of the Kolmogorov constant and intermittency exponent at very high Reynolds numbers. *Phys. Fluids.* **6,** 2886-2888.

PRASKOVSKY, A. A. & ONCLEY, S. 1994b Correlators of velocity differences and energy dissipation at very high Reynolds numbers. *Europhys. Lett.*, in press.

TSINOBER, A., KIT, E. & DRACOS, T. 1992 Experimental investigation of the field of velocity gradients in turbulent flows. *J. Fluid Mech.* **242,** 169-192.

WANG, L.-P., CHEN, S., BRASSEUR, J. G. & WYNGAARD, J. C. 1994 Examination of hypotheses in the Kolmogorov refined turbulence theory through high-resolution simulations. Submitted to *J. Fluid Mech.*